Porous Gelatin Membrane Obtained from Pickering Emulsions Stabilized by Graphene Oxide

Sakthivel Nagarajan, Dominique Abessolo Ondo, Sana Gassara, Mikhael Bechelany, Sebastien Balme, Philippe Miele, Narayana Kalkura, Céline Pochat-Bohatier

To cite this version:

Sakthivel Nagarajan, Dominique Abessolo Ondo, Sana Gassara, Mikhael Bechelany, Sebastien Balme, et al.. Porous Gelatin Membrane Obtained from Pickering Emulsions Stabilized by Graphene Oxide. Langmuir, 2018, 34 (4), pp.1542 - 1549. 10.1021/acs.langmuir.7b03426 . hal-01717296

HAL Id: hal-01717296
https://hal.umontpellier.fr/hal-01717296v1

Submitted on 4 Jun 2021

Porous Gelatin Membrane Obtained from Pickering Emulsions Stabilized by Graphene Oxide

Sakthivel Nagarajan [a,b]#, Dominique Abessolo Ondo [a]#, Sana Gassara[a], Mikhael Bechelany [a], Sebastien Balme [a]*, *Philippe Miele [a], Narayana Kalkura[b] and Celine Pochat-Bohatier [a]**

[a] Institut Européen des Membranes (IEM), University of Montpellier, CNRS, ENSCM, UMR 5635, Place Eugene Bataillon, 34095 Montpellier, France.

[b]Crystal Growth Centre, Anna University, Chennai, 600025, India.

* Corresponding authors : mikhael.bechelany@umontpellier.fr, Phone: +33467149167, Fax: +33467149119

Celine.pochat@umontpellier.fr, Phone: +33467143327, Fax: +33467149119

# **These two authors contributed equally to this paper**

ABSTRACT

This paper presents a novel procedure to prepare porous membranes from water-soluble polymers involving the formation of Pickering emulsion. Gelatin is a biodegradable biopolymer obtained by the partial hydrolysis of collagen. Biopolymer such as gelatin is capable to adsorb at oil/water interface and results to decrease interfacial energy. Hence, gelatin is widely employed as an alternate for synthetic surfactants to stabilize emulsions in food industry. However, high molecular weight gelatin leads to large emulsion droplets and poor emulsion stability. The amphoteric nature of graphene oxide (GO) nanosheets was helpful to stabilize the oil/water interface and allows preparing stable gelatin/GO emulsion. Membranes fabricated using gelatin/GO display uniformly distributed porous structure.

However, prepared membranes are highly hydrosoluble; hence the membranes were crosslinked without affecting their morphology. XRD results evidenced that gelatin effectively exfoliated the graphite oxide which is essential to stabilize the emulsion. Fabricated gelatin/GO membranes possess uniformly distributed pores and are highly stable in aqueous solution. Pure water filtration tests were conducted on the membranes. The permeability results proved that the membranes fabricated by Pickering emulsion are promising materials for filtration.

INTRODUCTION

Synthetic polymer based membranes are playing vital role in water separation and filtration industries. However, the manufacturing processes involve large organic solvents quantities which are toxic and costly in disposal. Developing membranes with bio-sourced polymers is an alternative to petroleum-based materials, due to renewable origin of raw materials. Attempts have been made to produce porous membranes from bio-source polymers but there are still many drawbacks to overcome [1, 2]. Many of them are water soluble on the contrary to synthetic polymers. A post-treatment to stabilize the structure is therefore necessary for applications in aqueous conditions. Temperature change during preparation process can induce strong modifications in their conformation (for instance physical gelation, starch gelatinization and retrogradation) [3, 4]. Because of these specific properties, it is not possible to transpose directly the usual processes to most of the bio-sourced polymer to form porous structure. Indeed, porous polymeric membranes are mainly prepared by processes inducing phase separation in polymer solution into two phases. The modulation of a thermodynamic parameter (e.g. solubility parameter, temperature) can induce the phase separation of a polymer solution which occurs to minimize the free energy of mixing.

Consequently a new equilibrium state is reached giving rise to a new structure [5, 6]. The polymer-rich phase solidifies quickly after the phase separation and forms the matrix of the membrane, whereas the polymer-poor phase gives the membrane pores.

Our group has already developed new membranes for gas separation operation using gelatin as bio-sourced polymers [7, 8]. Gelatin is obtained by controlled hydrolysis of collagen, a fibrous insoluble protein, which is widely found in nature as the major constituent of skin, bones and connective tissue. This biopolymer is extensively used in the food and pharmaceutical industry due to gelling and texturing properties. It is characterized by a complex structure. For gas separation, the membrane tailoring corresponds to the fabrication of structures displaying selective dense layers that are essential for gas sorption and diffusion. The next step in the development of gelatin-based membrane is to introduce controlled porous structure which is needed for fluids permeability. The idea developed in this paper is to produce gelatin emulsion and to stabilize it to give a porous structure, the continuous phase giving the membrane matrix whereas the dispersed phase will form the pores.

Various researchers prepared gelatin emulsion, and found that gelatin emulsions coalesce easily giving broadly distributed droplets size. Tan *et al.* prepared gelatin-stabilized high internal phase emulsion as nutraceutical containers and they found that the micron-sized pores were broadly distributed after cross-linking [9]. Lobo *et al.* also reported that gelatin is not as effective at formation of small drops compared to systems where surfactants are present. Additionally, nonionic surfactants are inefficient in stabilizing the gelatin emulsion [10]. Hence controlling the pore size and distribution and preserving the porous structure after the post processing treatment are essential to fabricate the gelatin based membranes. One of the novel methods that can be used to prepare porous structure is based on the preparation of a Pickering emulsion [11, 12]. Pickering emulsions are colloidal emulsions stabilized by solid nanoparticles adsorbed at Oil/Water interface instead of organic surfactants. Pickering emulsion stabilized using nanoparticles are benign to the environment in comparison to surfactants [13]. Variety of biocompatible nanoparticles synthesized using polymers, proteins and oxide based nanoparticles are successfully employed to stabilize the water/oil interface without using synthetic surfactants [14-16]. Solid stabilizing particles are necessarily smaller than emulsion droplets which are highly resistance to coalescence. The use of nanoparticles can help to control the pore distribution and add new interesting properties to the membrane.

The graphene oxide (GO) is composed of two dimensional nanosheets, obtained by the oxidative exfoliation of graphite [17, 18]. The GO is amphilic and display hydrophilic properties from the ionizable carboxylate, hydroxyl groups and hydrophobic properties from the carbon skeleton [19, 20]. The high surface area of the GO is also very helpful to stabilize the emulsion by reducing the interfacial energy. It also shows high affinity to aromatic solvent comparable than aliphatic solvent through π-π interaction. Hence the GO is a good emulsifier to stabilize aromatic solvent/gelatin emulsion to produce porous membranes [21, 22]. The GO nanoparticles were already employed to prepare Pickering emulsion. Tang *et al.* prepared polystyrene microspheres using graphene oxide/gold through Pickering emulsion process and used for the reduction of 4-nitrophenol [21]. He and his coworkers carried out a detailed analysis on various factors affecting graphene oxide Pickering emulsions [23]. Wan *et al.* prepared GO liquid crystals through Pickering emulsions [24]. The various researches on GO Pickering evidenced that the GO is a promising candidate to stabilize the Oil /Water interface [20] and environmentally benign material than commercially used surfactants.

Hence this paper reports for the first time a method to fabricate membranes displaying porous structure with gelatin using Pickering emulsion technique. The fabricated ~~produced~~ membranes are crosslinked using GTA without affecting the porous morphology and the crosslinked membranes are insoluble in water.

The stability of the cross-linked membranes in water was studied, and pure water permeability (PWP) measurements gave an evidence for the open porosity of material. This membrane preparation method using GO based Pickering emulsion could be appropriate for the fabrication of porous membranes from aqueous polymer solutions. The spontaneous demixing necessary in conventional phase separation process to form membrane porosity can be therefore induced in gelatin solution using this approach.

MATERIALS AND METHODS

1. Materials

Type B Gelatin (G9382) from bovine skin (gel strength 225 g Bloom), ethyl benzoate (E12907) (purification ≥99%, Mw=150 g mol^{-1} and density=1.045 g mL^{-1}), 25% glutaraldehyde (GTA) (G6257), Phosphoric acid (W290017), Sulfuric acid (258105), Graphite (28286), Potassium permanganate (223468) and Hydrogen peroxide (31642), were purchased from Sigma Aldrich and used without further purification.

2. Synthesis and purification of graphite oxide

The oxidation of graphite into graphite oxide was carried out using the improved protocol reported by Marcano *et al.* [25, 26]. Shortly, the acid mixture of H_2SO_4 and H_3PO_4 9:1 volume ratio respectively were prepared. The graphite (3 g) flakes are allowed to disperse in the prepared acid mixture and stirred for five minutes. 18 g of the $KMnO_4$ is carefully added by pinch into the graphite mixture and continued to agitate for 12 h, followed by the addition of 3 mL of 30% H_2O_2 to the mixture. The precipitates was centrifuged at 6000 RPM for 10 min and washed several times with 30% hydrochloric acid. The black colored supernatant evidences the dissolution of the insoluble salts. The washing must be repeated until clear supernatants are observed. The resultant brown color precipitates are washed with 200 mL of ethanol and dried at 50°C for 24 h to obtain the pure graphite oxide.

3. Membrane preparation

GO suspensions were prepared by the addition of graphite oxide in water with a concentration of 1, 3 and 6 g.L^{-1} and dispersed by sonication with an ultrasonic probe system (SONOPULS HD 3100, 100 W, 20 kHz) for 10 minutes (9 second pulse on and 3 second off) with 45% amplitude. Gelatin solution (22% W/V) was prepared by dissolving gelatin in graphene oxide (0, 1, 3 and 6 g.L^{-1}) aqueous suspension under magnetic stirring at 35°C. The ethyl benzoate (EthB) was added into the as-prepared GO-gelatin suspensions with a volume ratio (O/W) of 0.6. The emulsions were prepared by sonication with the same equipment for 7 minutes (9 second pulse on and 2 second off) with 45 % amplitude. Samples were stored in water bath at 45°C and cast onto a support with an initial thickness of 500 µm. Then a first set of uncross-linked membranes were obtained after dry casting at 37°C for 4 days. The choice of an aromatic organic solvent like EthB as oil phase was governed by the facts that (*i*) it is almost insoluble in water, (*ii*) miscible with most organic solvents in particular ethanol and (*iii*) emulsions are well stabilized by graphene oxide nanoparticles.

4. Membrane cross-linking

A second set of membranes was prepared for cross-linking. In that case, the duration of the drying step was reduced to 12 h. The membranes were cross-linked by direct immersion in 0.5% glutaraldehyde (GTA) solution prepared from 25% GTA stock solution, using 96% ethanol as a solvent. The membranes were kept in the GTA solution at 37°C for 5 h. This step enables also ethyl benzoate extraction. Additional washing of membranes was conducted in ethanol and water bathes. Then the membranes were dried again for 12 h.

The membranes using 1 g.L^{-1}, 3 g.L^{-1} and 6 g.L^{-1} of graphene oxide suspensions are hereafter denoted as GGO1, GGO3 and GGO6. These membranes were cross-linked with 0.5% GTA and hereafter denoted as GGO1-R, GGO3-R and GGO6-R. The membranes prepared from EthB in gelatin emulsion without graphene oxide are denoted GGO0 and GGO0-R which are uncrosslinked and crosslinked respectively. The crosslinked membranes were dried at 50 °C and used for further characterization after drying.

5. Membrane characterization

5.1. Structural and chemical characterizations

The morphology of the membrane cross-section and surface has been observed using a HITACHI S4800 scanning electron microscopy system. The samples were first coated with platinum using ion sputter coater. Water contact angles were measured using a monochrome camera B-CAM-21-BW (CCCIR) and a Led R60 lamp purchased from CONRAD. For each sample, 10.0 µL of ultrapure water was deposited on a polymer coated microscope slide using a needle. The images were recorded by One Touch Grabber software and treated using Image J® software. The XRD patterns of crosslinked gelatin/ GO membranes were recorded using PANalytical Xpert powder XRD system with CuKα radiation, scan speed of 2° min^{-1}, 2θ ~~Θ~~ range between 3-70°, and step rate 0.02° per second. The FTIR spectra of uncrosslinked and crosslinked gelatin/GO membranes were recorded by NEXUS instrument, equipped with an attenuated total reflection (ATR) accessory in the frequency range of 600-4000 cm^{-1}. The FTIR spectra were recorded at 4 cm^{-1} resolution and the signals were averaged from 32 scans. GO (3mg~~/~~.mL^{-1}) suspension was prepared using deionized water and sonicated (SONOPULS HD 3100, 100 W, 20 kHz) for 10 minutes. Mechanical properties of the cross-linked gelatin and gelatin/GO membranes were characterized using the dynamic mechanical analysis system

(Metravib 50N) at the tensile testing speed (cross head speed) of 0.4 mm.min^{-1}. Young's modulus of the membranes was calculated from elastic region of the stress-strain graphs.

5.2. Swelling kinetics

The films were cut in 2x2 cm² pieces and dried at 37°C during 24 h. The initial weight of the membranes are recorded and equilibrated at ambient temperature in 3 ml of deionized water. The swelling kinetics were evaluated periodically by measuring the weight of the films using a micro-balance (Sartorius CPA225D, with an accuracy of 0.00001 g), after gently blotting the surface with a tissue.

The swelling ratio was evaluated as:

$$SWR = \frac{weight\ film\ - weight\ dry\ film}{weight\ dry\ film}$$

All data shown are the average value of three replicates.

5.3. Permeability measurements

Frontal filtration experiments were carried out using a stirred dead-end cell (Amicon 8050, Millipore Corporation) with a membrane active surface area of 13.4 cm^2. The membranes were first compacted by filtering pure water up to 3.4 bar until a constant flux was observed. Pure water flux (J_{PW}) was measured for each membrane by circulating pure water through the membrane system using an applied pressure range of 0–3 bar.

J_{PW} (l m^{-2} h^{-1}) was calculated using the following formula:

$$J_{PW} = \frac{Q}{\Delta t.A}$$

where Q (l) is amount of water collected, Dt (h) time duration using a membrane of area A (m^2). Pure water permeability (PWP) was determined from the slope of the linear variation of J_{PW} versus the applied pressure.

5.4. Pore size determination

Two techniques were used to characterize the membrane pore size and their distribution: (1) processing the SEM images obtained with a magnification of x400 using the Image J® software and (2) Liquid–gas displacement porometry. The measurements were carried using a porometer PRM-2000-LL-R (IFTS-France). In that method, the pores of the sample were first filled with water during a wetting step. Then, a flow rate of nitrogen gas is applied through the membrane and was measured as a function of the applied pressure. When a straight line is obtained between nitrogen flow and pressure, all pores have been opened. Calculation of pore dimension patterns is made by applying Poiseuille's Law. All data shown are the average value of three replicates.

RESULTS AND DISCUSSION

1. Synthesis and characterization of gelatin membranes:

Gelatin is already well-known for its ability to stabilize emulsion so the first membranes were prepared using EthB-in-gelatin-solution. The SEM micrographs (Figure 1) displays the cross-section of uncross-linked and cross-linked gelatin membranes (without GO). Big ellipsoidal macro-voids (Figure 1 red arrow) are present before cross-linking, whereas the structure is collapsed after cross-linking. This phenomenon can be explained by the GTA cross-linking reaction in ethanol solution. Indeed, the cross-linking step has been conducted in GTA/ethanol solution for 5 h, enabling ethyl benzoate extraction and GTA diffusion in the membrane pores. GTA is a small molecule with two aldehyde groups, separated by a flexible chain of three methylenes. The mechanism for the cross-linking of gelatin by glutaraldehyde is pH dependent and very complex [27]. In this work, we used type B gelatin which has an isoelectric pH between 4.7 and 5.2. The gelatin solutions had a pH close to 6 and the red color of ethyl benzoate with ethyl red indicator shows the pH between 4.4 and 6.2 (Figure 1 (inset image)). The pKa of residual amine group values arginine and lysine (~13%) in gelatin is greater than 9, which clearly shows that the nucleophilic addition type of reaction by amine groups of gelatin with GTA is not favorable. However, stability of the membranes in aqueous solution (Figure 6(a)) evidences the cross-linking, whereas, uncross-linked membranes are soluble. Cross-linking is due to the nucleophile attack of hydroxyl group from hydroxyproline on GTA as proposed by Farris *et al.* [27]. It should be noticed that gelatin contains ~27% of hydroxyproline and proline.

The uncross-linked gelatin membrane morphology displays irregular voids (Figure 1a (GGO0)), with large distribution of macro-voids. It is due to the coalescence of gelatin emulsion during casting and drying steps. Indeed, it has been reported that gelatin solutions exhibit low adsorption efficiency compared to surfactants. Its effectiveness of stabilizing emulsion depends strongly on its molecular mass fractions [28]. Gelatin which displays a molecular mass distribution with a high content of low molecular mass is more efficient for stabilizing emulsions [28]. In this work, gelatin was chosen with medium molecular weight (40-50 kDa) suitable for emulsion stabilization but also suitable for membrane preparation. The surfactant properties of gelatin depends on it amino-acids composition. According to Lin *et al.*, the gelatin is composed of around 7% of the amino acids with aliphatic residue (leucine, isoleucine and valine) which can be mainly involved in hydrophobic interaction with an interface [29]. The contribution of these hydrophobic groups should be involved in adsorption process at the oil/water interface and the drop size reduction. A study on coalescence during emulsification conducted by Lobo showed that gelatin yielded larger oil drops, leading to modest reduction in surface tension when compared to anionic surfactants. Therefore, gelatin is not very effective for the formation of small droplets, compared to other surfactants [10]. With the aim of characterizing the filtration ability of the as-prepared membranes, the surface morphology was observed by SEM (Figure 1a). Uncross-linked and cross-linked EthB/gelatin membranes display collapsed pores (Figure 1a) which is inadequate for filtration operations. Indeed membranes for filtration should possess bulk porous structure along with numerous pores at the surface.

The membrane preparation process was thus modified to produce membranes with more homogeneous pore distribution as well as increase pore number at the surface. Lobo indicated that nonionic surfactants are very inefficient for stabilizing droplets in a gelatin containing system [10]. Here we have used graphene oxide (GO) to stabilize EthB-in-gelatin emulsion by producing Pickering emulsion, and the cast solution was dried to obtain porous membranes.

2 Preparation and characterizations of EthB/ GO emulsion

The characterization of the GO wettability was performed by measuring water contact angle on thin GO film deposit onto a glass microscope slide (Figure 2). The water contact angle (ca. 36°) demonstrate hydrophilic character for GO. The GO particle surface tends therefore to reside more in water than in oil and will stabilize rather O/W emulsions. He *et al.* demonstrated that the stabilizing ability of GO for aromatic solvents was much greater than that for non-aromatic solvents [23]. This was explained by the π-π interactions between the residual conjugate domains in GO and the aromatic molecules. On the basis of the work of He *et al.* ethyl benzoate was chosen as oil phase because it is not classified as dangerous according to the REACH (Registration, Evaluation, Authorization and restriction of Chemicals) regulation [23]. Spontaneous demixing system is crucial to fabricate membranes. In general, phase separation induced by non-solvent addition or temperature change in homogeneous polymer solution is employed. Gelatin/water system employed in this study possesses poor demixing property. Hence, O/W spontaneous demixing system was designed to facilitate membrane fabrication. However, stabilizing of the emulsion droplet is crucial to engineer the pore size and membrane physical properties which can be effectively controlled using Pickering emulsion technique. Graphene oxide was dispersed in water without gelatin at three different concentrations: 1, 3 and 6 g.L^{-1} for the purpose to observe the effect of GO concentration on the droplet size (GO1, GO3 and GO6 respectively). EthB-in-water Pickering emulsions were then produced by using sonication and then observed by optical microscopy. As shown in Figure 2, the GO concentration has a strong influence on the average droplets size as well on the emulsion stability. At low GO concentration, the droplets become bigger by coalescence phenomenon. However, an increase of GO concentration induces a reduction of the droplets coalescence as observed in GO6. With respect to the low water contact angle of GO thin film, the latter is hydrophilic. Thus, it suggests that a part of GO is dispersed in the aqueous phase and another part is located at the O/W interface. When graphene oxide concentration is raised from 1 to 6 g.L ^{1}, more particles can migrate from the aqueous phase to O/W interface, reducing the surface energy of the interface. The reduction of the surface energy of the interface makes it more stable and leads to smaller average droplets size as observed on Figure 2. Direct observation of EthB-in-gelatin solution emulsion stabilized by GO were not successful because of the gelation of the system on the microscope slide.

3 Synthesis and Characterization of gelatin/GO membranes

The oxidation of graphite into graphite oxide and exfoliation of graphite oxide into graphene oxide through gelatin/Graphite oxide interaction was confirmed using XRD patterns. The XRD patterns of graphite oxide, gelatin/GO crosslinked membranes are shown in the Figure 3. The broadband of gelatin between 15 to 20° evidences the amorphous nature of gelatin

[30]. The (002) planes of graphite oxide, as shown in the Figure 3, depicts the complete oxidation of graphite. Distance between the adjacent layer is calculated which is found to be 8.4 A° and evidenced the graphite exfoliation. The (002) plane of graphite oxide disappears for gelatin/GO membranes (GGO1-R, GGO3-R, GGO6-R), which shows that the graphite oxide is exfoliated into GO [31, 32]. The presence of carboxylate and hydroxyl groups on GO supports its dispersion in gelatin through hydrogen bonding. The exfoliated few layered GO nanosheets plays important role in Pickering emulsion to stabilize the water/oil interface.

3.1 Effect of cross-linking on membrane morphology

GO was used to stabilize the EthB-in-gelatin emulsion and form Pickering emulsion, but also to prevent membrane collapsing after cross-linking treatment. It has been showed in Figure 2 that without any gelatin, GO stabilizes successfully the emulsion and prevents droplet coalescence especially when graphene oxide concentration reaches 6 g~~1~~L^{-1} (Figure (2) (GGO6)). However, understanding the emulsion droplet size of gelatin/GO is limited due to its gelling nature at ambient temperature. However, higher temperature leads to coalescence of emulsion droplets. First a set of SEM observations on uncross-linked membrane surface and cross-section has been realized (Figure 4). The same observations were realized on cross-linked membranes.

These two sets of SEM micrographs clearly show that the cross-linking treatment in Ethanol/GTA bath modifies the membrane microstructure whatever the GO concentration. For low graphene oxide concentration (1 g.L^{-1}), the membrane surface displays few pores which are suppressed after cross-linking (Figure 4 (GGO1-R)). The ethanol used to prepare the GTA solution induces a rupture of inter and intra molecular hydrogen bonds between water and gelatin resulting in a reorganization of the gelatin chains. This phenomenon proceeds in two steps: (i) a selective charge neutralization and (ii) a gain in entropy induced by a random mixing of gelatin and the release of counter ions.[33] These effects could facilitate the overall shrinkage of the membranes. The 3 g.L $^{-1}$ graphene oxide dispersed in gelatin (GGO3) controls the shrinkage of pores and maintains the porous structure (Figure 4). It evidences that the GO nanosheets controls the shrinkage of gelatin. The 3 g.L $^{-1}$ graphene oxide acts as an intermediate concentration with rather big surface pores (GGO3). The increase of the graphene oxide concentration (6 g.L $^{-1}$) decreases the size of the emulsion as evidenced from the Figure 3b. Hence, higher concentration (6 g.L $^{-1}$) of laterally micron sized GO leads to fold around gelatin and results to lamellar like porous morphology on cross-linking as evidenced from the SEM micrograph (Figure 4, GGO6-R cross section).

The oxidation of graphite, the interaction of gelatin/GO and the effect of cross-linking on gelatin structure were analyzed by FTIR and are shown in Figure 5 (a,b). The FTIR graph of raw gelatin shows the amide I C=O stretching and the amide II N-H bending bands at 1628, 1530 cm^{-1}, respectively [34]. The FTIR spectrum of graphite oxide shows the C=O stretching band of carbonyl and carboxylic group at 1729 and 1618 cm^{-1}, respectively [35]. The strong absorption peak of uncrosslinked gelatin and gelatin/GO (GGO1-R, GGO3-R, GGO6-R) samples at 1275 (C-O), 1106 and 709 cm^{-1} are characteristic stretching modes of ethyl benzoate, which disappear after cross-linking (Figure 5(b)). The EthB disappears after cross-linking, which evidences that ethanol used to prepare the cross-linking solution extracts the ethyl benzoate from the membranes as shown by the red arrow (Figure 5 (a)).

3.2 Swelling and mechanical properties of gelatin/GO membranes.

The swelling capacity of crosslinked gelatin and gelatin/GO membranes in water was measured and shown in the Figure 6(a). The gelatin is highly water soluble, hence cross-linking the membranes is essential for long term application of the membranes. The uncrosslinked gelatin membranes show uncontrollable swelling which leads to the dissolution of gelatin and disintegrates the membranes in less than 1 hour. Hence, the gelatin and gelatin/GO membranes were crosslinked and the intermolecular covalent interaction of gelatin permit to avoid its dissolution. Indeed, the crosslinked gelatin/GO membranes with GTA show stability in water for at least 325 h. In addition, the cross-linkage permits to obtain a swelling ratio (SWR) between 1 and 3. It is difficult to point out a direct correlation between GO concentration and maximum SWR.

Mechanical properties of the composites are analyzed and shown in the Figure 6(b) and Table 1 in order to evaluate the effect of GO addition. Linear elastic region of the stress/strain graph for the composites are utilized to calculate the Young’s modulus. Surprisingly, mechanical properties such as young’s modulus, tensile stress at break and tensile strain at break show that GO addition does not affect the mechanical properties. This can be explained by the influence of the membrane porous structure on the mechanical properties which overcomes the GO effect.

4. Permeability measurements

The ability of these porous membranes to filtrate water was characterized by determining the flux versus pressure. The flux is determined by the specific resistance of the membrane material under a given differential pressure across the membrane, so that the flux increases with the operating area of the membrane and with the applied pressure. Thus, experiments conducted at different pressures allow the determination of the pure water permeability (*PWP*) of the as-prepared membranes. It was not possible to calculate *PWP* for GGO0-R and GGO1-R membranes because the fluxes were really too low to be measured and reflected only diffusion phenomena through the top dense layer of the membrane. As it can be seen on Figure 1 and on Figure 4, the surface layers porosity is hardly visible. A dense top layer on the porous membrane prevents filtration ability of the structure. Concerning GGO3-R and

GGO6-R membranes, filtration experiments allowed to determine the values of permeability which were 5.8 ± 1.3 L h^{-1} m^{-2} bar^{-1} and 0.3 ± 0.1 L h^{-1} m^{-2} bar^{-1}. The higher *PWP* value obtained with GGO3-R membranes has to be related to its bigger surface pores as clearly shown by SEM micrographs (**Erreur ! Source du renvoi introuvable.**).

The mean pore diameter and the pore size distribution at the surface for these membranes were determined by processing the obtained SEM images using the Image J® software and with liquid-gas porometer, the results were presented and summarized in Figure 7 and Table 2, respectively. The pore size distribution obtained by SEM is larger than the one given by the porometer. This can be explained by the swelling of the gelatin along the wetting step for porosimetry measurement which reduces the void between the cell walls of the porous structure. On the contrary, the polymer is dehydrated for SEM observation and the cell walls are thinner. Additionally, the determination of the pore size and the pore size distribution directly on SEM micrographs are local measurements whereas porometry analyzes wider surfaces. Thus, GGO3-R membranes display mean pore size of 1.6 ± 0.5 µm whereas GGO6-R of 0.6 ± 0.1 µm as determined by liquid-gas porometry, in wet state. This pore size range characterizes microfiltration membranes [36]; however the *PWP* is very low. This can be explained by a bad interconnection between pores as depicted on Figure S1 (Supporting Information).

CONCLUSION

In this work, porous gelatin membranes were successfully developed using a new process based on the preparation of EthB-in-gelatin solution emulsion stabilized by GO using Pickering emulsion concept. It has been shown that porous membranes could be already prepared using emulsion and without GO addition. Nevertheless, these membranes presented irregular porous structure because of a likely non-controlled coalescence phenomena.

Moreover, this structure was collapsing after cross-linking with GTA which is an essential step to avoid gelatin dissolution in water. The porous structure collapsing was evidenced by SEM observation but also because the obtained membranes were unable to filtrate water. The addition of GO stabilized the emulsion thanks to amphoteric nature of the graphene oxide which stabilizes the EthB phase through π-π interaction. This leads to stable emulsion with smaller average droplets. In addition, the optimal concentration ($3\ \mathrm{g.\ L^{-1}}$) of GO stabilizes the porous surface and place important role in maintaining the morphology even after cross-linking. The higher concentration ($6\ \mathrm{g.L^{-1}}$) of GO shows porous lamellar structure, due to big lateral size of GO folding. Finally, experiments with membranes prepared with $3\ \mathrm{g.\ L^{-1}}$ GO have demonstrated that they were stable in water for more than 13 days and they could give *PWP* value*s* up to $5.8 \pm 1.3\ \mathrm{L\ h^{-1}\ m^{-2}\ bar^{-1}}$. This new membrane preparation procedure is therefore promising to develop microfiltration membranes but efforts must be made to improve the membrane performance, by raising the number of pore connections.

ACKNOWLEDGMENTS

The work was financially supported by the French National Agency (ANR) through the LabEx CheMISyst (ANR-10-LABX-05-01). S. N. benefits from Svagaata Fellowship (Erasmus Mundus Program, European Union).

REFERENCES

[1] Meireles IT, Brazinha C, Crespo JG, Coelhoso IM. A new microbial polysaccharide membrane for ethanol dehydration by pervaporation. Journal of Membrane Science 2013;425–426:227-34.
[2] Moriya A, Maruyama T, Ohmukai Y, Sotani T, Matsuyama H. Preparation of poly(lactic acid) hollow fiber membranes via phase separation methods. Journal of Membrane Science 2009;342:307-12.
[3] Fredriksson H, Silverio J, Andersson R, Eliasson AC, Åman P. The influence of amylose and amylopectin characteristics on gelatinization and retrogradation properties of different starches. Carbohydrate Polymers 1998;35:119-34.
[4] Ross-Murphy SB. Special issue: 2nd International Workshop on Plant PolysaccharidesPhysical gelation of biopolymers. Food Hydrocolloids 1987;1:485-95.

[5] Mulder M. Preparation of Synthetic Membrane, in: Basic Principles of Membrane Technology. Kluwer Academic Publishers 1991:55-109.
[6] van de Witte P, Dijkstra PJ, van den Berg JWA, Feijen J. Phase separation processes in polymer solutions in relation to membrane formation. Journal of Membrane Science 1996;117:1-31.
[7] Biscarat J, Charmette C, Sanchez J, Pochat-Bohatier C. Preparation of dense gelatin membranes by combining temperature induced gelation and dry-casting. Journal of Membrane Science 2015;473:45-53.
[8] Biscarat J, Bechelany M, Pochat-Bohatier C, Miele P. Graphene-like BN/gelatin nanobiocomposites for gas barrier applications. Nanoscale 2015;7:613-8.
[9] Tan H, Sun G, Lin W, Mu C, Ngai T. Gelatin Particle-Stabilized High Internal Phase Emulsions as Nutraceutical Containers. ACS Applied Materials & Interfaces 2014;6:13977-84.
[10] Lobo L. Coalescence during Emulsification. Journal of Colloid and Interface Science 2002;254:165-74.
[11] Charmette C, Sanchez J, Gramain P, Masquelez N. Structural characterization of poly(ethylene oxide-co-epichlorohydrin) membranes and relation with gas permeation properties. Journal of Membrane Science 2009;344:275-80.
[12] Charmette C, Sanchez J, Gramain P, Rudatsikira A. Gas transport properties of poly(ethylene oxide-co-epichlorohydrin) membranes. Journal of Membrane Science 2004;230:161-9.
[13] Tang M, Wu T, Xu X, Zhang L, Wu F. Factors that affect the stability, type and morphology of Pickering emulsion stabilized by silver nanoparticles/graphene oxide nanocomposites. Materials Research Bulletin 2014;60:118-29.
[14] Jin W, Zhu J, Jiang Y, Shao P, Li B, Huang Q. Gelatin-Based Nanocomplex-Stabilized Pickering Emulsions: Regulating Droplet Size and Wettability through Assembly with Glucomannan. Journal of Agricultural and Food Chemistry 2017;65:1401-9.
[15] Yang Y, Fang Z, Chen X, Zhang W, Xie Y, Chen Y, et al. An Overview of Pickering Emulsions: Solid-Particle Materials, Classification, Morphology, and Applications. Frontiers in Pharmacology 2017;8.
[16] Wu J, Ma G-H. Recent Studies of Pickering Emulsions: Particles Make the Difference. Small 2016;12:4633-48.
[17] Le TXH, Bechelany M, Lacour S, Oturan N, Oturan MA, Cretin M. High removal efficiency of dye pollutants by electron-Fenton process using a graphene based cathode. Carbon 2015;94:1003-11.
[18] Inagaki M, Kang F. Graphene derivatives: graphane, fluorographene, graphene oxide, graphyne and graphdiyne. Journal of Materials Chemistry A 2014;2:13193-206.
[19] Dreyer DR, Park S, Bielawski CW, Ruoff RS. The chemistry of graphene oxide. Chemical Society Reviews 2010;39:228-40.
[20] Kim J, Cote LJ, Kim F, Yuan W, Shull KR, Huang J. Graphene Oxide Sheets at Interfaces. Journal of the American Chemical Society 2010;132:8180-6.
[21] Tang M, Wang X, Wu F, Liu Y, Zhang S, Pang X, et al. Au nanoparticle/graphene oxide hybrids as stabilizers for Pickering emulsions and Au nanoparticle/graphene oxide@polystyrene microspheres. Carbon 2014;71:238-48.
[22] Montes-Navajas P, Asenjo NG, Santamaría R, Menéndez R, Corma A, García H. Surface Area Measurement of Graphene Oxide in Aqueous Solutions. Langmuir 2013;29:13443-8.
[23] He Y, Wu F, Sun X, Li R, Guo Y, Li C, et al. Factors that Affect Pickering Emulsions Stabilized by Graphene Oxide. ACS Applied Materials & Interfaces 2013;5:4843-55.
[24] Wan W, Zhao Z, Hughes TC, Qian B, Peng S, Hao X, et al. Graphene oxide liquid crystal Pickering emulsions and their assemblies. Carbon 2015;85:16-23.
[25] Marcano DC, Kosynkin DV, Berlin JM, Sinitskii A, Sun Z, Slesarev A, et al. Improved Synthesis of Graphene Oxide. ACS Nano 2010;4:4806-14.
[26] Le TXH, Bechelany M, Champavert J, Cretin M. A highly active based graphene cathode for the electro-fenton reaction. RSC Advances 2015;5:42536-9.
[27] Farris S, Song J, Huang Q. Alternative Reaction Mechanism for the Cross-Linking of Gelatin with Glutaraldehyde. Journal of Agricultural and Food Chemistry 2010;58:998-1003.

[28] Müller HJ, Hermel H. On the relation between the molecular mass distribution of gelatin and its ability to stabilize emulsions. Colloid and Polymer Science 1994;272:433-9.
[29] Lin S-Y, Wu T-F, Tsao H-K. Interfacial Dynamics of a Gelatin Solution with Surfactant. Macromolecules 2003;36:8786-95.
[30] Tomšová K, Ďurovič M, Drábková K. The effect of disinfection methods on the stability of photographic gelatin. Polymer Degradation and Stability 2016;129:1-6.
[31] Han D, Yan L, Chen W, Li W. Preparation of chitosan/graphene oxide composite film with enhanced mechanical strength in the wet state. Carbohydrate Polymers 2011;83:653-8.
[32] Piao Y, Chen B. One-pot synthesis and characterization of reduced graphene oxide-gelatin nanocomposite hydrogels. RSC Advances 2016;6:6171-81.
[33] Mohanty B, Bohidar HB. Systematic of Alcohol-Induced Simple Coacervation in Aqueous Gelatin Solutions. Biomacromolecules 2003;4:1080-6.
[34] Payne KJ, Veis A. Fourier transform ir spectroscopy of collagen and gelatin solutions: Deconvolution of the amide I band for conformational studies. Biopolymers 1988;27:1749-60.
[35] Xie G, Cheng J, Li Y, Xi P, Chen F, Liu H, et al. Fluorescent graphene oxide composites synthesis and its biocompatibility study. Journal of Materials Chemistry 2012;22:9308-14.
[36] Mulder J. Basic principles of Membrane technology. 2 ed: Springer Netherlands; 1996.

FIGURES

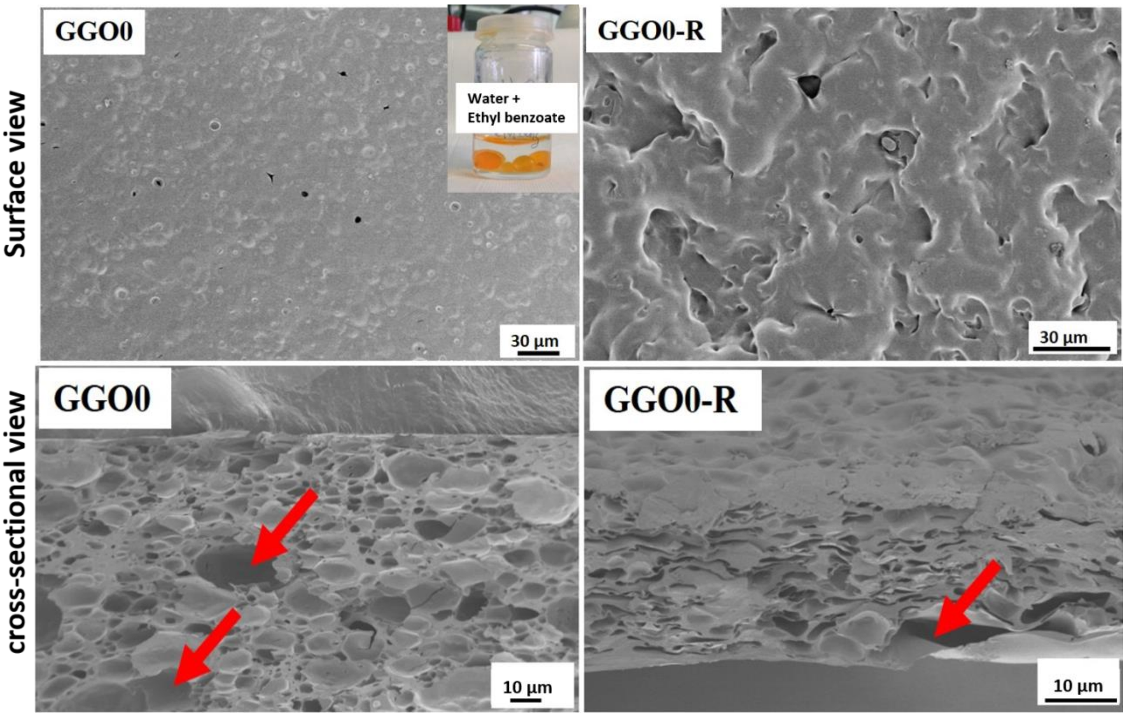

Figure 1. The surface and cross sectional SEM images of uncrosslinked gelatin/EthB and cross-linked gelatin/EthB membranes. Arrows indicate macrovoids, inset image is ethyl benzoate in water (methyl red was added to ethyl benzoate, giving evidence of a pH between 4.4 and 6.2).

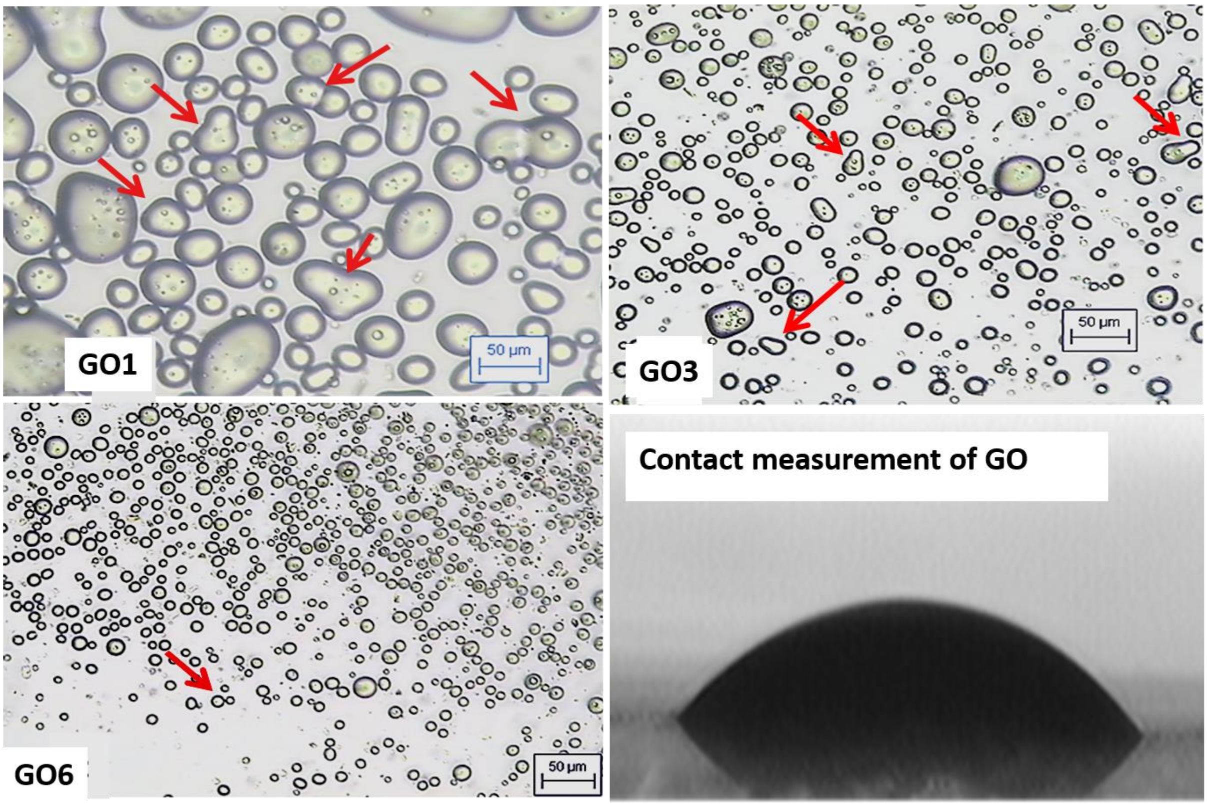

Figure 2. Optical micrographs of EthB-in-water Pickering emulsions stabilized by GO. (Arrows indicate coalescence phenomena in case of GO1 and GO3, but it can be seen that for GO6 droplets can stand close without coalescing) and Water contact angle measurement of GO.

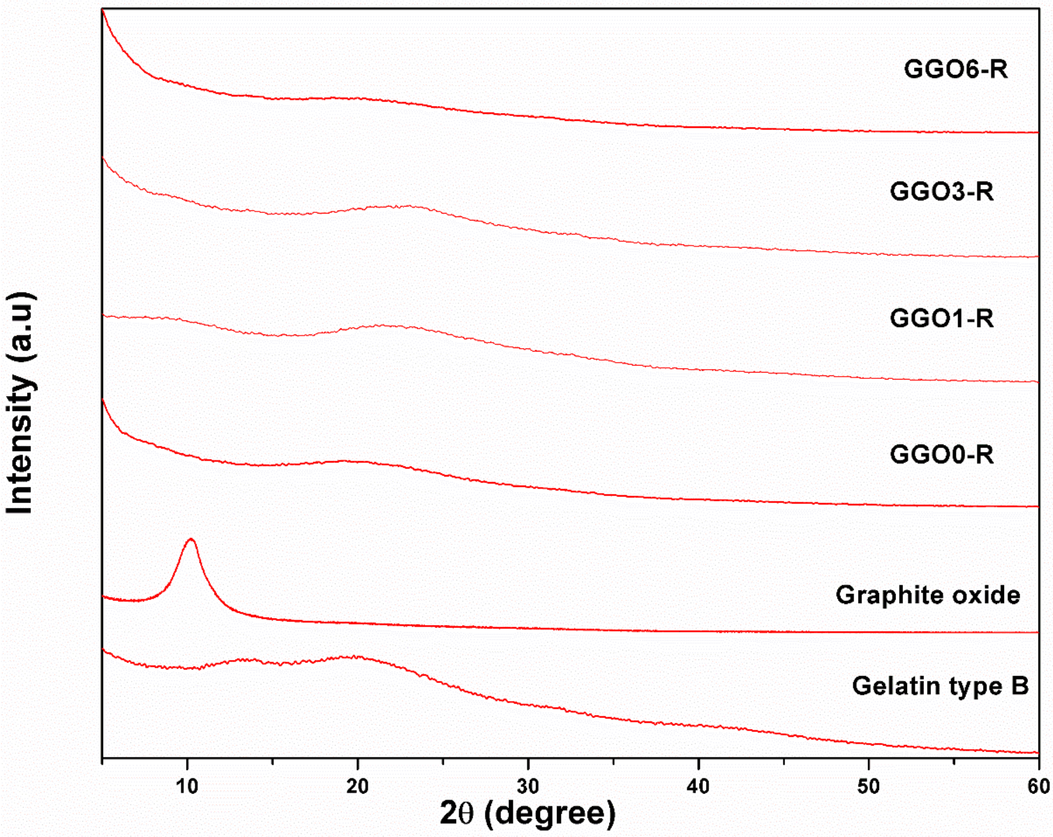

Figure 3. XRD patterns of crosslinked gelatin/GO membranes.

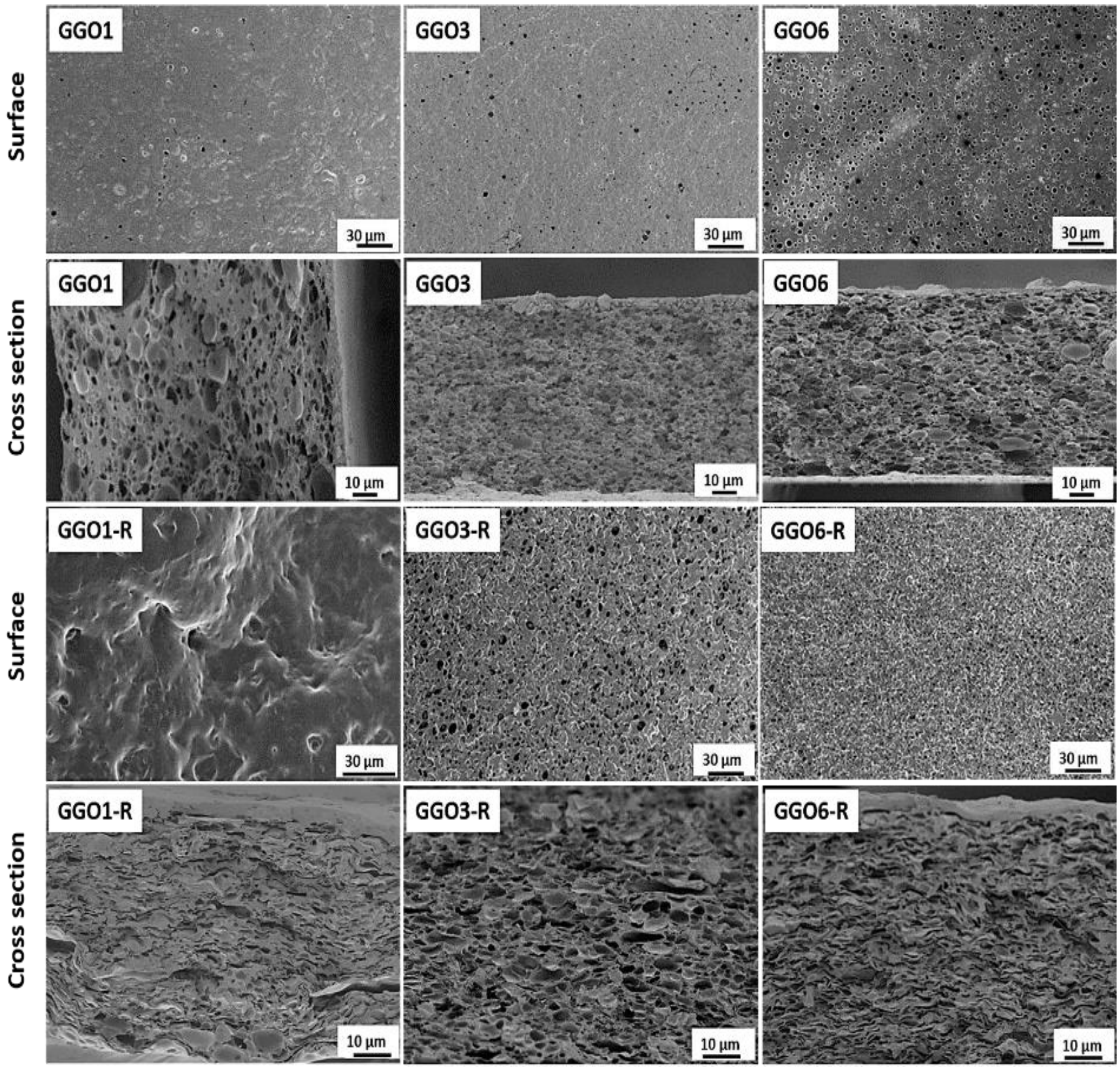

Figure 4. SEM observations of uncrosslinked and crosslinked gelatin and gelatin/GO membranes.

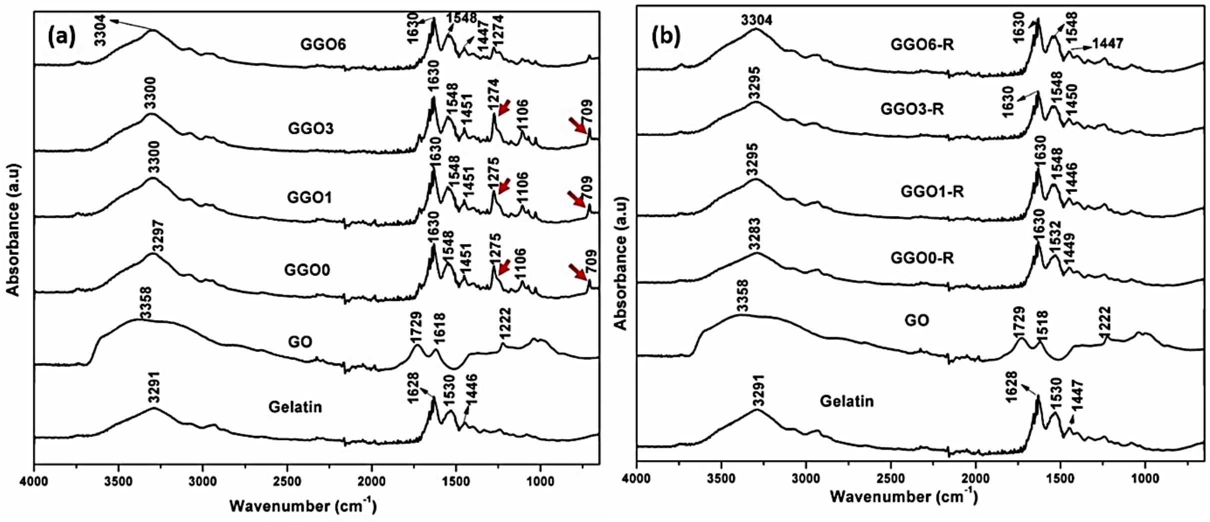

Figure 5. FTIR spectrum of (a) uncrosslinked and (b) crosslinked membranes (Red arrow indicates the extraction of ethyl benzoate).

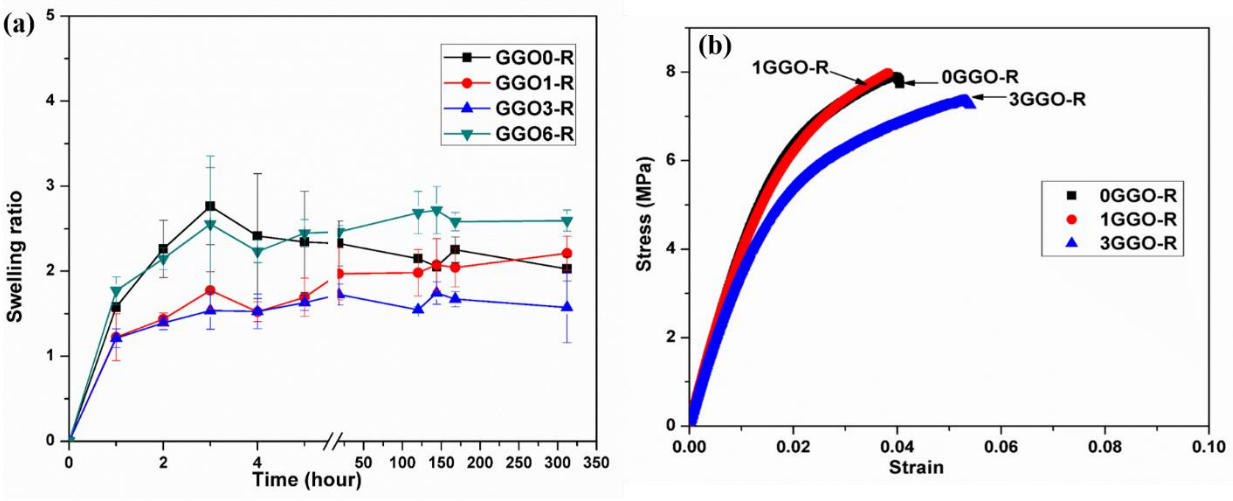

Figure 6. (a) Swelling ratio and (b) Mechanical properties of crosslinked gelatin and gelatin/GO membranes.

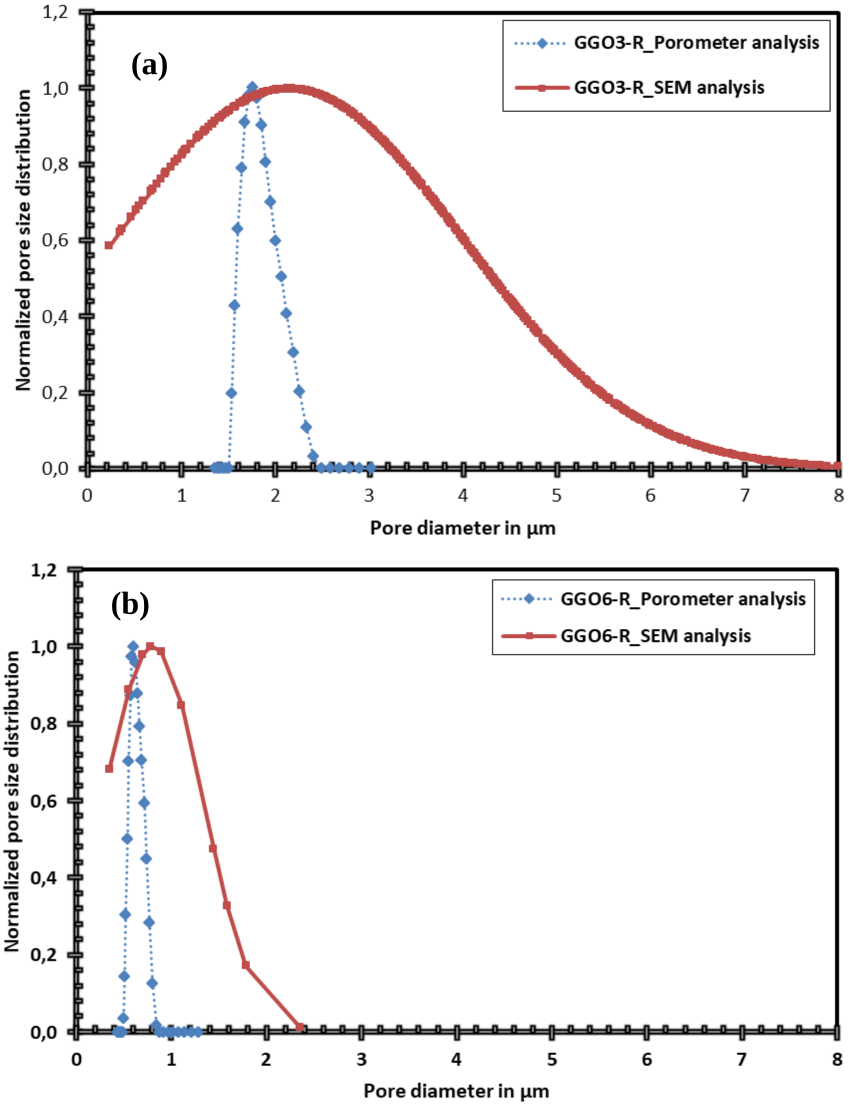

Figure 7. Pore size distributions determined by SEM and liquid-gas porometry analyses of: (a) GG03-R membrane and (b) GG06-R membrane.

TABLES

Table 1. Mechanical properties of the Gelatin/GO membranes.

Sample	Tensile Stress at break (MPa)	Strain (%)	Young's Modulus (MPa)
GGO0-R	8.11 ± 1.51	4.01 ± 0.77	488 ± 76
GGO1-R	7.35 ± 2.08	3.46 ± 1.16	426 ± 57
GGO3-R	8.28 ± 1.03	7.23 ±1.90	430 ± 77

Table 2. Geometric mean pore size diameter (dp) for GG03-R and GG06-R membranes obtained by SEM images and liquid–gas displacement porometry.

Method	Mean pore size diameter ± Standard deviation (μm)	
	GG03-R membrane	GG06-R membrane
SEM	2.1 ± 1.8	0.8 ± 0.5
Liquid–gas porometry	1.6 ± 0.5	0.6 ± 0.1

TOC GRAPHIC